

W.L. Murphy^{1,4}, C.A. Simmons^{1,2,4},
D. Kaigler², and D.J. Mooney^{1,2*,3}

¹Department of Biomedical Engineering, ²Department of Biologic and Materials Sciences, and ³Department of Chemical Engineering, University of Michigan, 5213 Dental, 1011 North University Avenue, Ann Arbor, MI 48109-1078; ⁴contributed equally; *corresponding author, mooneyd@umich.edu

J Dent Res 83(3):204-210, 2004

ABSTRACT

Angiogenesis and biomineral substrates play major roles in bone development and regeneration. We hypothesized that macroporous scaffolds of biomineralized 85:15 poly(lactide-co-glycolide), which locally release vascular endothelial growth factor-165 (VEGF), would direct simultaneous regeneration of bone and vascular tissue. The presence of a bone-like biomineral substrate significantly increased regeneration of osteoid matrix ($32 \pm 7\%$ of total tissue area; mean \pm SD; $P < 0.05$) and mineralized tissue ($14 \pm 2\%$; $P < 0.05$) within a rat cranium critical defect compared with a non-mineralized polymer scaffold ($19 \pm 8\%$ osteoid and $10 \pm 2\%$ mineralized tissue). Further, the addition of VEGF to a mineralized substrate significantly increased the generation of mineralized tissue ($19 \pm 4\%$; $P < 0.05$) compared with mineralized substrate alone. This appeared to be due to a significant increase in vascularization throughout VEGF-releasing scaffolds (52 ± 9 vessels/mm²; $P < 0.05$) compared with mineralized scaffolds without VEGF (34 ± 4 vessels/mm²). Surprisingly, there was no significant difference in total osteoid between the two samples, suggesting that increased vascularization enhances mineralized tissue generation, but not necessarily osteoid formation. These results indicate that induced angiogenesis can enhance tissue regeneration, supporting the concept of therapeutic angiogenesis in tissue-engineering strategies.

KEY WORDS: tissue engineering, VEGF, hydroxyapatite, poly(lactide-co-glycolide), drug delivery.

Bone Regeneration via a Mineral Substrate and Induced Angiogenesis

INTRODUCTION

Contemporary approaches to materials design for tissue regeneration mimic particular components of the natural tissue development microenvironment to direct growth of a single tissue type. These schemes generally involve implantation of a synthetic extracellular matrix (ECM) (Putnam and Mooney, 1996), sustained delivery of a growth factor or plasmid DNA to induce tissue regeneration (Richardson *et al.*, 2001a), or transplantation of cells capable of generating neo-tissue (Ohgushi and Caplan, 1999). More recent studies combining multiple constituents of natural tissue (*i.e.*, combination of natural ECMs and precursor cells) into single biomaterial scaffolds have led to extensive regeneration of particular tissue types, such as bone tissue (Bonadio *et al.*, 1999; Krebsbach *et al.*, 2000; Petite *et al.*, 2000). These studies are promising, and suggest the possibility of engineering functional organ replacements. However, organs contain multiple tissue types, which often require distinct stimuli to direct their regeneration. Therefore, approaches to regenerate complex, three-dimensional organs (*e.g.*, bone, tooth) are likely to require simultaneous presentation of distinct stimuli within a single material construct.

A common material theme of emerging bone regeneration approaches is the creation of an environment that mimics bone ECM (Hartgerink *et al.*, 2001), which is composed mainly of a carbonate hydroxyapatite (cHAP) biomineral component interspersed within a collagen I framework. Despite difficulties associated with inadequate pore interconnectivity and inefficient or incomplete resorption *in vivo*, materials composed of biominerals can serve as outstanding substrates for bone tissue ingrowth and differentiation of transplanted bone-forming cells (Ohgushi and Caplan, 1999; Petite *et al.*, 2000). Current bone regeneration strategies have not actively and specifically attempted, however, to promote the invasion of blood vessels and the formation of a vascular network (angiogenesis) within the forming tissue, processes essential to bone development. The vasculature provides for the mass transport requirements of the tissue (Colton, 1995), may deliver circulating stem cells that can participate in bone formation (Prockop, 1997), and facilitates cross-talk between endothelial cells and pre-osteoblasts to direct their differentiation (Villars *et al.*, 2000). A variety of growth factors that direct angiogenesis has been identified, including vascular endothelial growth factor (Deckers *et al.*, 2002). VEGF-mediated angiogenesis has recently been shown to direct bone tissue formation at sites of endochondral ossification (Gerber *et al.*, 1999).

We hypothesized that a synthetic system capable of presenting an osteoconductive surface and delivering an angiogenic growth factor in a localized and sustained manner would direct simultaneous regeneration of bone and vascular tissue. A biomineral coating was created on the surfaces of three-dimensional, porous poly(lactide-co-glycolide) scaffolds *via* a biomimetic approach to serve as an osteogenic substrate, and VEGF-165 was incorporated into the scaffolds for localized delivery. This scaffold

system may also prove applicable to other bone regeneration approaches, such as those that incorporate bone-forming stem cells or osteogenic growth factors (e.g., bone morphogenetic proteins, BMPs). Previous studies in cranial defect models have shown that BMPs have a positive effect on bone regeneration (Ono *et al.*, 1992; Arnaud *et al.*, 1999; Han *et al.*, 2002), and the system we describe herein could readily be designed to release these factors in a localized, sustained manner. In addition, the general concept of combining signals that affect growth of complementary tissue types (*i.e.*, bone and vascular tissue) into a single scaffold vehicle may have wide utility in directing tissue regeneration.

MATERIALS & METHODS

Materials

Poly(lactide-co-glycolide) (PLG) (Medisorb 85:15, Intrinsic Viscosity = 0.8 dl/g) was from Alkermes (Cincinnati, OH, USA). VEGF 165 was from Intergen (Purchase, NY, USA), and ^{125}I -VEGF was from New England Nuclear (Boston, MA, USA). Sodium alginate was from ProNova (Oslo, Norway). All chemicals were from Fisher Scientific (Springfield, NJ, USA) or Sigma (St. Louis, MO, USA) unless noted otherwise. Immunostaining for von Willebrand Factor (vWF) used a rabbit anti-human vWF (A0082) primary antibody and biotinylated anti-rabbit IgG (K1498 rabbit line) from DAKO (Carpinteria, CA, USA).

Scaffold Fabrication and *in vitro* Characterization

Scaffolds were formed with the use of a gas-foaming/particulate-leaching process, as described (Richardson *et al.*, 2001b). We modified the previous protocol by hydrolyzing the PLG particles ($106\ \mu\text{m} < d < 250\ \mu\text{m}$) *via* a 10-minute incubation in 0.5 M NaOH prior to inclusion in the gas-foaming/particulate-leaching process. The hydrolysis functionalizes the PLG surfaces with carboxylic acid and hydroxyl groups that induce heterogeneous biomineral growth (Murphy and Mooney, 2002). Hydrolysis had no appreciable effect on the diameter or mass of PLG particles, confirmed *via* sieve separation and mass measurements (> 98% particulate retrieval efficiency).

Biomineral growth was accomplished on some scaffolds *via* a five-day incubation in a modified simulated body fluid (mSBF), as described previously (Murphy and Mooney, 2002). Lyophilized

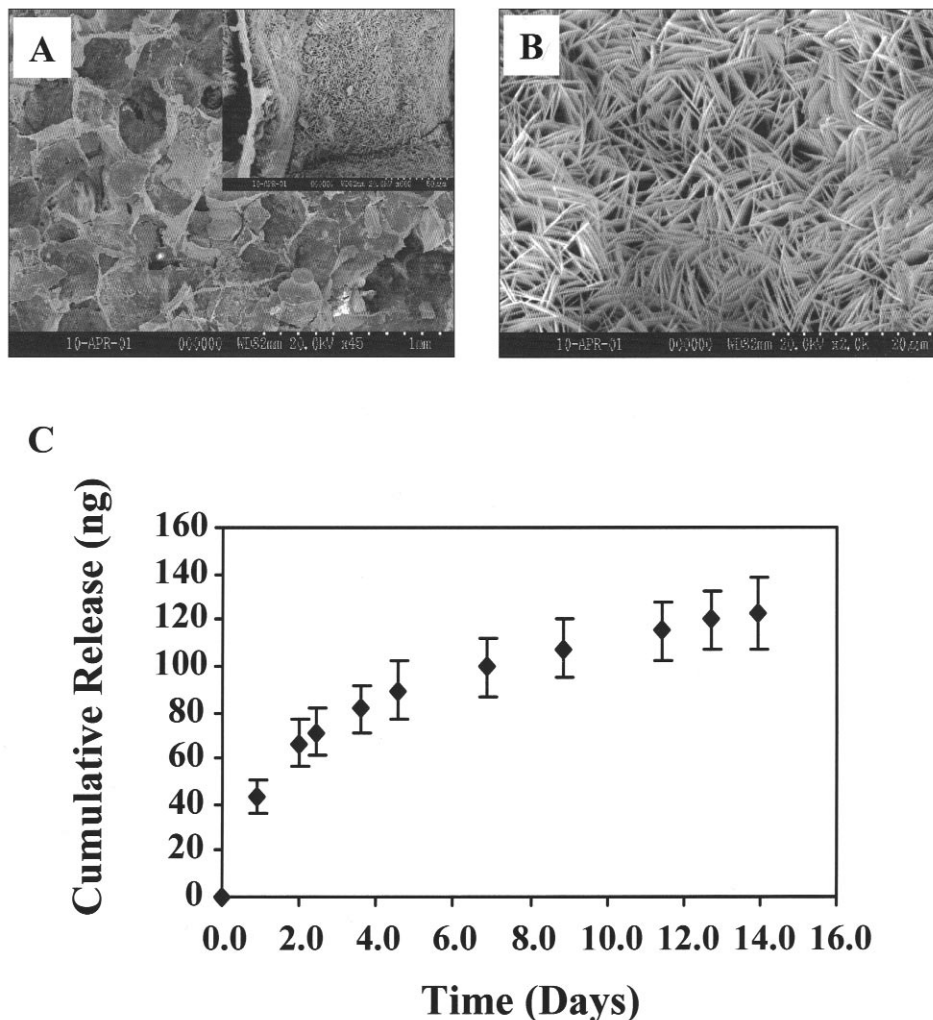


Figure 1. Imaging of mineralized scaffolds and measurement of VEGF release kinetics. **(A)** Electron micrographs displaying 85:15 PLG scaffolds with an interconnected pore structure ($250 < d < 425\ \mu\text{m}$). Scale bar = 1 mm. **(A, inset)** The surface of a single pore within the scaffold coated with a thin biomineral film (scale bar = $60\ \mu\text{m}$). **(B)** The biomineral film displays a platelike nanostructure similar to that of native bone mineral (scale bar = $20\ \mu\text{m}$). Biomineralization was achieved *via* incubation of pre-hydrolyzed scaffolds in mSBF for 5 days. **(C)** *In vitro* release kinetics of VEGF from mineralized scaffolds. Data in plot represent mean \pm standard deviation ($n = 5$).

and Au-coated scaffolds were analyzed with the use of a Hitachi S-3200N scanning electron microscope with an energy-dispersive x-ray detector (Noran SiLi) for elemental analysis of mineral crystals. We determined *in vitro* VEGF release kinetics by placing scaffolds (diameter = 4.2 mm, thickness = 2.5 mm) fabricated with $0.5\ \mu\text{Ci}$ ^{125}I -VEGF as a tracer into PBS following fabrication and mineralization.

Rat Cranium Critical Defect Model

University of Michigan and National Institutes of Health animal care guidelines were followed. Scaffolds were implanted into a critical-sized defect created in the crania of anesthetized Lewis rats. After we cleared the periosteum from the cranial surface by scraping, we used a trephine bur to create a circular 9-mm-diameter defect in the cranium. The full thickness (~ 1.5 -2 mm) of the cranial bone was removed, and a mineralized scaffold (diameter = 9 mm, thickness = 2 mm) \pm VEGF or a non-

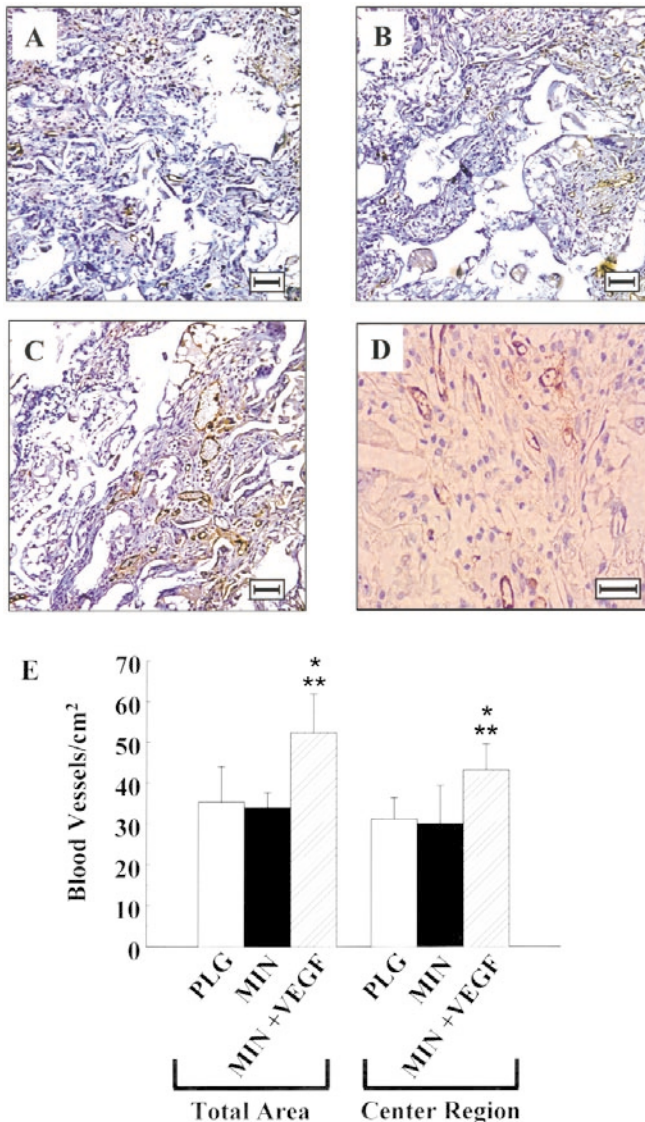


Figure 2. VEGF release enhances blood vessel ingrowth 2 wks post-implantation. (A-D) vWF immunostaining of blood vessels within sections of implanted PLG (A), mineralized PLG (B), and VEGF-releasing, mineralized PLG (C) scaffolds. Positive vWF staining is brown, and circular vWF staining represents a blood vessel. (D) Higher-magnification image of a different region within a VEGF-releasing, mineralized PLG scaffold. (E) Quantification of blood vessel densities within the total scaffold area and a region in the center of the scaffold for each condition. *P < 0.01 relative to the PLG condition; **P < 0.01 relative to the mineralized PLG condition (n = 4 for MIN; n = 6 for PLG and MIN + VEGF). Data in plot represent mean \pm standard deviation. Scale bars = 100 μ m (in A-C) or 20 μ m (in D). Sections were counterstained with hematoxylin.

mineralized control scaffold was immediately placed in the defect. After 2 or 14 wks, the animals were killed, and the implants were retrieved and fixed for 24 hrs at 4°C in 10% zinc-buffered formalin. Following fixation, implants were either plastic-embedded and sectioned (14-week implants) or decalcified *via* incubation in 10% EDTA, paraffin-embedded, and sectioned (two-week samples).

Analysis of Blood Vessel Ingrowth

Two-week tissue sections were immunostained for vWF, a protein present in large quantities in subendothelial matrices such as blood vessel basement membranes (Ruggeri and Savage, 1998), and imaged by means of a Nikon Eclipse E800 light microscope and a Spot RT digital camera (Diagnostic Instruments, Sterling Heights, MI, USA). Blood vessels, indicated by vWF staining, were counted manually at 100X magnification in the total scaffold area and in a 1.5-mm² region in the center of the scaffold area, and normalized to tissue area with the use of Image Pro Plus Software (Media Cybernetics, Carlsbad, CA, USA).

Analysis of Bone Regeneration

Bridging of the defects with tissue was examined 14 wks post-implantation in sections stained with hematoxylin and eosin (H&E). To confirm that the 9-mm defect was critical-sized, we created a defect without implanting a scaffold and observed no spontaneous bridging of the defect 8 wks post-implantation. Previous studies have shown no spontaneous bridging of 8-mm cranial defects at 13 mos (Hollinger and Kleinschmidt, 1990). Fourteen-week non-demineralized tissue sections were stained with Goldner's Trichrome stain for osteoid or von Kossa stain for mineralized tissue according to routine protocols and imaged digitally at 100X magnification. Osteoid and fully mineralized tissue were identified throughout the entire implant, and the tissue areas, as a fraction of the total tissue area, were computed.

Statistical Analysis

Four to six scaffolds were prepared, implanted, and analyzed *per* condition. In some cases, one sample *per* condition was not quantitatively analyzed due to an aberration (*e.g.*, death of an animal). Data in graphs represent means and standard deviations. Histomorphometric data were analyzed by ANOVA, with pairwise comparisons made by one-tailed SNK tests.

RESULTS

Scaffold Formation and *in vitro* Analysis

To present both an osteoconductive substrate signal and an angiogenic signal within a single delivery material, we developed an approach to fabricate biomineralized growth-factor-releasing scaffolds. The biomineral film formed by this process covered much of the inner pore surface of the scaffold (Figs. 1a, 1b) and was comprised of plate-like, nanoscale crystals (Fig. 1b). This mineral was similar in structure to bone mineral, and had an elemental composition (Ca/P = 1.55) in the range of biological apatites. The scaffolds in which VEGF was incorporated contained 3 μ g VEGF after salt leaching and mineralization, and the incorporated VEGF was released in a sustained manner over 14 days *in vitro* (Fig. 1c).

Induction of Angiogenesis

To determine the effects of sustained VEGF delivery on blood vessel ingrowth in a bone defect model, we implanted scaffolds into critical-sized cranial defects in Lewis rats. The densities of blood vessels present in PLG (P) scaffolds, mineralized PLG (MP) scaffolds, and mineralized, VEGF-releasing PLG (MVP) scaffolds were measured 2 wks post-implantation. Histological sections stained for vWF showed relatively few blood vessels within P and MP scaffolds (Figs. 2a, 2b). In contrast, MVP scaffolds displayed a high density of blood vessels interspersed

throughout the scaffold (Fig. 2c, 2d). Quantification of blood vessel densities throughout the total scaffold area confirmed that MVP scaffolds had a significantly higher blood vessel density than P and MP scaffolds (Fig. 2e). Strikingly, the center region deep within MVP scaffolds also contained a higher density of blood vessels than the center regions of P or MP scaffolds (Fig. 2e). The center regions of all scaffold types had lower blood vessel densities than the periphery, as expected.

Bone Tissue Regeneration

The effects of biomineral presence and induced angiogenesis on bone tissue regeneration within the critical-sized defects after 14 wks were next analyzed. In contrast to an untreated defect, which showed only minimal appositional bone regeneration and a thin layer of fibrous tissue (Fig. 3a), the defects treated with an MVP scaffold were nearly completely bridged with tissue (Fig. 3b). Bridging of the defect area with tissue appeared similar at low magnification for all three experimental conditions (data not shown). Whereas the interface between the native bone and implant was primarily fibrous tissue within control scaffolds (Fig. 3c), regions resembling bone tissue were evident in both MP and MVP scaffolds in this region (Figs. 3d, 3e). Subsequently, these tissues were stained more specifically for the presence of osteoid matrix and mineralized tissue, for confirmation of bone tissue ingrowth within the scaffold. Histological analysis indicated that there were small regions of osteoid matrix within the interior of the control scaffolds (Fig. 3f) and a larger amount of osteoid in each of the experimental conditions (Figs. 3g, 3h). Histomorphometric analysis corroborated the histological findings, showing a significantly higher osteoid fractional area within MP and MVP scaffolds

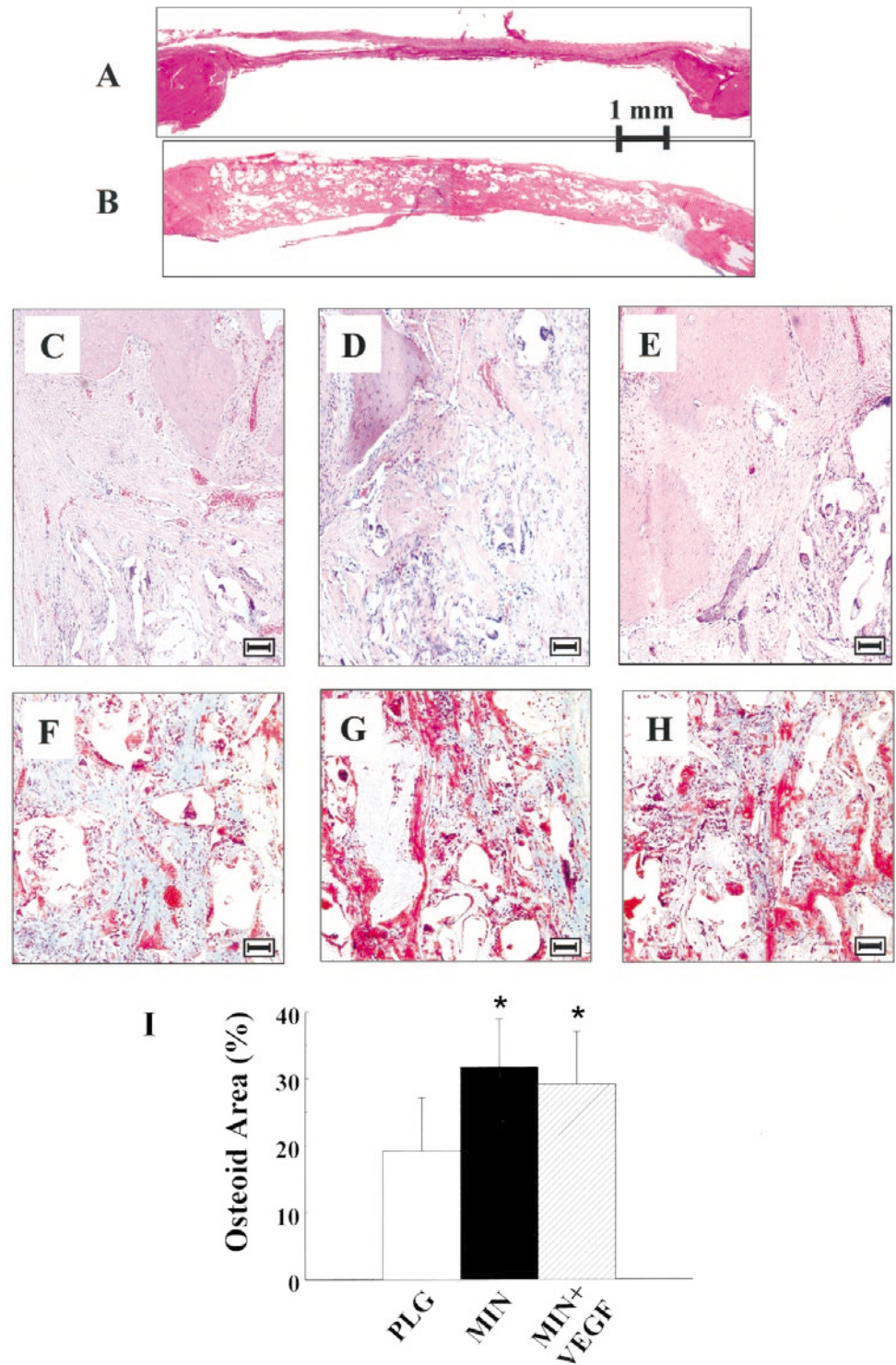


Figure 3. Mineralized scaffolds support enhanced bone tissue ingrowth, and biomineral presence significantly enhances osteoid matrix deposition. (A,B) Hematoxylin and eosin (H&E) staining of sections of a critical-sized defect without an implanted scaffold (A) and a defect after implantation of a mineralized, VEGF-releasing PLG scaffold (B). Bridging of the defect area with tissue was evident for all three experimental conditions (data not shown). (C-E) Higher-magnification H&E staining of implanted PLG (C), mineralized PLG (D), and VEGF-releasing, mineralized PLG (E) scaffolds 14 wks postimplantation. (F-H) Goldner's trichrome staining of implanted PLG (F), mineralized PLG (G), and VEGF-releasing, mineralized PLG (H) scaffolds 14 wks post-implantation (red = osteoid matrix). (I) Quantification of osteoid matrix fractional area within the scaffold area for each condition. *P < 0.05 relative to the PLG condition (n = 5 for PLG and MIN; n = 6 for MIN + VEGF). Data in plot represent mean ± standard deviation. Scale bar = 1 mm (in A-B) or 100 µm (in C-H).

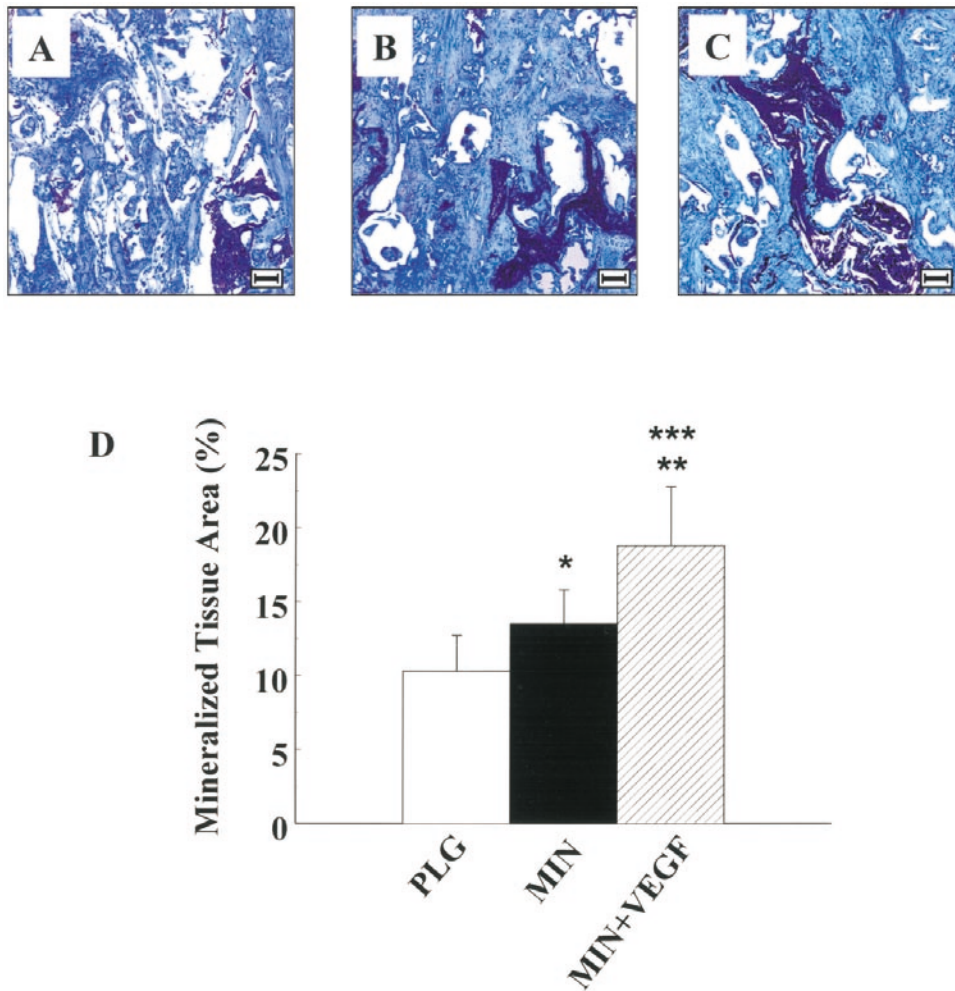


Figure 4. Biomaterial presence and induced angiogenesis concertedly enhance mineralized tissue regeneration. (A-C) von Kossa staining of implanted PLG (A), mineralized PLG (B), and VEGF-releasing, mineralized PLG (C) scaffolds 14 wks post-implantation (dark purple-black = mineralized tissue) displaying bone regeneration in the interior of the scaffold. (D) Quantification of mineralized tissue fractional area within the scaffold area for each condition. * $P = 0.065$ relative to the PLG condition; ** $P < 0.01$ relative to the PLG condition; *** $P < 0.01$ relative to the mineralized PLG condition ($n = 5$ for PLG and MIN; $n = 6$ for MIN + VEGF). Data in plot represent mean \pm standard deviation. Scale bars = 100 μm .

relative to control scaffolds (Fig. 3i). Similarly, small regions of mineralized tissue were evident within the interior of control scaffolds (Fig. 4a), while a larger amount of mineralized tissue was present in each of the experimental conditions (Figs. 4b, 4c). Histomorphometric analysis confirmed that the mineralized tissue fractional area was greater within MP and MVP scaffolds than within P scaffolds (Fig. 4d). Importantly, there was a statistically significant increase in mineralized tissue fractional area within MVP scaffolds when compared with MP scaffolds, indicating that induced angiogenesis leads to more complete mineralized tissue regeneration within the defect area.

DISCUSSION

Engineering of complex, three-dimensional tissues will likely benefit from approaches that more closely mimic natural tissue regeneration processes, combining multiple, complementary

signals into a single regeneration vehicle. This study demonstrates that a physical substrate signal that mimics natural bone ECM and a biochemical soluble signal that induces rapid growth of a vascular supply concertedly enhance bone regeneration in a critical-sized bone defect model. Sustained VEGF delivery induces significant blood vessel ingrowth during the early stages of bone regeneration in this system. Ultimately, mineralized, VEGF-releasing scaffolds cause a 62% increase in the fractional area of regenerated bone tissue (osteoid + mineralized tissue) when compared with polymer scaffolds alone. The results of this study exhibit the complementary importance of insoluble and soluble signals in tissue regeneration, and highlight the potential utility of multifaceted approaches in engineering simultaneous regeneration of multiple tissue types.

This study supports previous evidence that biomaterial substrata enhance osteoconductivity and provide a favorable substrate for infiltration and function of osteogenic cell types. The mineral substrate alone produces a striking effect on bone regeneration, with a 53% increase in the total bone tissue fractional area compared with non-mineralized polymer scaffolds. This result is consistent with those of previous bone regeneration studies of the

rat cranial defect model (Marden *et al.*, 1993; Krebsbach *et al.*, 2000). While other materials developed to mimic the mineral phase of bone tissue (*i.e.*, sintered porous hydroxyapatite scaffolds, coralline matrices, hydroxyapatite bone cements) can be effective, they are often entirely composed of mineral, have inadequate pore interconnectivity, and typically degrade incompletely, even over very long time scales. In contrast, the biomaterial film grown in this study is a thin surface component of a degradable, organic scaffold with a highly interconnected pore structure, potentially circumventing problems associated with resorption and pore interconnectivity. The continued presence of polymer scaffold interspersed in the defect at the time points studied was expected, since the PLG utilized to fabricate the scaffolds degrades on the order of months (Vert *et al.*, 1992). We chose this PLG composition to eliminate the variable of polymer degradation during regeneration in this study, but a more rapidly degrading PLG may be readily used

in this system. Importantly, the mineral coating the PLG is carbonated, calcium-deficient, and poorly crystalline (Murphy and Mooney, 2002), similar to human bone mineral (Posner, 1969), and has a higher solubility product ($K_{sp} = 10^{-69}$) (data not shown) than stoichiometric hydroxyapatite ($K_{sp} = 10^{-117}$) (Oonishi and Oomamiuda, 1998) in physiological buffer.

The results of this study support the concept that angiogenesis can enhance bone regeneration. Localized and sustained VEGF delivery improves fully mineralized tissue regeneration but, at the time point observed in this study, does not substantially enhance the presence of osteoid matrix when compared with a biomineral substrate alone. This suggests that angiogenesis speeds the differentiation and/or maturation of infiltrating osteoblasts and osteoblast precursor cells during neo-bone development, perhaps by providing a conduit for delivery of osteoinductive soluble signals. The effects of VEGF delivery observed in this study corroborate those from recent work that highlights the importance of VEGF and induced angiogenesis in endochondral ossification (Gerber *et al.*, 1999) and normal fracture healing (Hausman *et al.*, 2001). Although cranial defects undergo intramembranous rather than endochondral ossification, induction of angiogenesis in the rat cranium may similarly invoke infiltration of osteoblasts and endothelial cells that are essential for bone morphogenesis. Recent studies also indicate that VEGF may enhance migration and differentiation of osteoblasts (Mayr-Wohlfart *et al.*, 2002; Street *et al.*, 2002), and that VEGF is essential for regeneration of bone tissue (Street *et al.*, 2002). Thus, the effects of VEGF delivery on bone regeneration presented herein may also be partially attributed to the direct influence of VEGF on osteoblast differentiation. It is noteworthy that our strategy to promote bone regeneration *via* induced angiogenesis could be particularly important in larger-sized defects, in which the presence of a vascular supply is perhaps more vital. In addition, rapid angiogenesis may improve transplanted cell survival in cell-based tissue-engineering strategies, leading to more complete regeneration of large volumes of tissue.

Natural development and regeneration of organs involve a complex interplay between multiple signal types, leading to coordinated growth of multiple tissue types (Gilbert, 2000). These signals are often presented by the natural ECM, which simultaneously presents substrate signals and sequesters soluble components (*e.g.*, growth factors) for localized signaling. Similarly, complex tissue-engineering schemes will likely require presentation of multiple signals from a matrix to enhance and coordinate growth of complementary tissues. We have now shown that simultaneous delivery of an ECM cue and an inductive soluble signal within a porous construct leads to simultaneous regeneration of both vascular tissue and bone tissue. This approach mimics the multifunctionality of the ECM in bone and other tissues, and these results have implications for other regeneration schemes that necessitate growth of multiple tissue types *via* presentation of complementary signals.

ACKNOWLEDGMENTS

The authors acknowledge technical support from Amru Albeiruty, Ralph Dilisio, and Charisa Roy, and financial support from the National Institutes of Health (RO1 DE 13033

to D.J.M., and T32 GM 08353 to W.L.M.) and the Natural Sciences and Engineering Research Council of Canada (post-doctoral Fellowship to C.A.S.).

REFERENCES

- Arnaud E, De Pollak C, Meunier A, Sedel L, Damien C, Petite H (1999). Osteogenesis with coral is increased by BMP and BMC in a rat cranioplasty. *Biomaterials* 20:1909-1918.
- Bonadio J, Smiley E, Patil P, Goldstein S (1999). Localized, direct plasmid gene delivery in vivo: prolonged therapy results in reproducible tissue regeneration. *Nat Med* 5:753-759.
- Colton CK (1995). Implantable biohybrid artificial organs. *Cell Transplant* 4:415-436.
- Deckers MM, van Bezooijen RL, van der Horst G, Hoogendam J, van Der Bent C, Papapoulos SE, *et al.* (2002). Bone morphogenetic proteins stimulate angiogenesis through osteoblast-derived vascular endothelial growth factor A. *Endocrinology* 143:1545-1553.
- Gerber HP, Vu TH, Ryan AM, Kowalski J, Werb Z, Ferrara N (1999). VEGF couples hypertrophic cartilage remodeling, ossification and angiogenesis during endochondral bone formation. *Nat Med* 5:623-628.
- Gilbert SF (2000). Developmental biology. 6th ed. Sunderland, MA: Sinauer Associates.
- Han B, Perelman N, Tang B, Hall F, Shors EC, Nimni ME (2002). Collagen-targeted BMP3 fusion proteins arrayed on collagen matrices or porous ceramics impregnated with Type I collagen enhance osteogenesis in a rat cranial defect model. *J Orthop Res* 20:747-755.
- Hartgerink JD, Beniash E, Stupp SI (2001). Self-assembly and mineralization of peptide-amphiphile nanofibers. *Science* 294:1684-1688.
- Hausman MR, Schaffler MB, Majeska RJ (2001). Prevention of fracture healing in rats by an inhibitor of angiogenesis. *Bone* 29:560-564.
- Hollinger JO, Kleinschmidt JC (1990). The critical size defect as an experimental model to test bone repair materials. *J Craniofac Surg* 1:60-68.
- Krebsbach PH, Gu K, Franceschi RT, Rutherford RB (2000). Gene therapy-directed osteogenesis: BMP-7-transduced human fibroblasts form bone in vivo. *Hum Gene Ther* 11:1201-1210.
- Marden LJ, Quigley NC, Reddi AH, Hollinger JO (1993). Temporal changes during bone regeneration in the calvarium induced by osteogenin. *Calcif Tissue Int* 53:262-268.
- Mayr-Wohlfart U, Waltenberger J, Hausser H, Kessler S, Gunther KP, Dehio C, *et al.* (2002). Vascular endothelial growth factor stimulates chemotactic migration of primary human osteoblasts. *Bone* 30:472-477.
- Murphy WL, Mooney DJ (2002). Bioinspired growth of crystalline carbonate apatite on biodegradable polymer substrata. *J Am Chem Soc* 124:1910-1917.
- Ohgushi H, Caplan AI (1999). Stem cell technology and bioceramics: from cell to gene engineering. *J Biomed Mater Res* 48:913-927.
- Ono I, Ohura T, Murata M, Yamaguchi H, Ohnuma Y, Kuboki Y (1992). A study on bone induction in hydroxyapatite combined with bone morphogenetic protein. *Plast Reconstr Surg* 90:870-879.
- Oonishi H, Oomamiuda K (1998). Degradation/resorption in bioactive ceramics in oopaedics. In: Handbook of biomaterial properties. Black J, Hastings G, editors. London: Chapman & Hall, pp. 406-419.

- Petite H, Viateau V, Bensaid W, Meunier A, de Pollak C, Bourguignon M, *et al.* (2000). Tissue-engineered bone regeneration. *Nat Biotechnol* 18:959-963.
- Posner AS (1969). Crystal chemistry of bone mineral. *Physiol Rev* 49:760-792.
- Prockop DJ (1997). Marrow stromal cells as stem cells for nonhematopoietic tissues. *Science* 276:71-74.
- Putnam AJ, Mooney DJ (1996). Tissue engineering using synthetic extracellular matrices. *Nat Med* 2:824-826.
- Richardson TP, Murphy WL, Mooney DJ (2001a). Polymeric delivery of proteins and plasmid DNA for tissue engineering and gene therapy. *Crit Rev Eukaryot Gene Expr* 11:47-58.
- Richardson TP, Peters MC, Ennett AB, Mooney DJ (2001b). Polymeric system for dual growth factor delivery. *Nat Biotechnol* 19:1029-1034.
- Ruggeri ZM, Savage B (1998). Structure and biosynthesis of von Willebrand factor. In: von Willebrand factor and the mechanisms of platelet function. Ruggeri ZM, editor. Georgetown: Springer and R.G. Landes Company, pp. 79-109.
- Street J, Bao M, deGuzman L, Bunting S, Peale FV Jr, Ferrara N, *et al.* (2002). Vascular endothelial growth factor stimulates bone repair, by promoting angiogenesis and bone turnover. *Proc Natl Acad Sci USA* 99:9656-9661.
- Vert M, Li S, Garreau H (1992). New insights on the degradation of bioresorbable polymeric devices based on lactic and glycolic acids. *Clin Mater* 10:3-8.
- Villars F, Bordenave L, Bareille R, Amedee J (2000). Effect of human endothelial cells on human bone marrow stromal cell phenotype: role of VEGF? *J Cell Biochem* 79:672-685.